The Plant Cell, Vol. 28: 2212–2224, September 2016, www.plantcell.org

Dynamic Interactions of Arabidopsis TEN1: Stabilizing Telomeres in Response to Heat Stress

Jung Ro Lee,[a,1] Xiaoyuan Xie,[a] Kailu Yang,[a] Junjie Zhang,[a] Sang Yeol Lee,[b] and Dorothy E. Shippen[a,2]

[a] Department of Biochemistry and Biophysics, Texas A&M University, College Station, Texas 77843-2128
[b] Division of Applied Life Sciences (BK21+) and PMBBRC, Gyeongsang National University, Jinju 52828, Republic of Korea

ORCID ID: 0000-0002-5030-9810 (X.X.)

Telomeres are the essential nucleoprotein structures that provide a physical cap for the ends of linear chromosomes. The highly conserved CST (CTC1/STN1/TEN1) protein complex facilitates telomeric DNA replication and promotes telomere stability. Here we report three unexpected properties of *Arabidopsis thaliana* TEN1 that indicate it possesses functions distinct from other previously characterized telomere proteins. First, we show that telomeres in *ten1* mutants are highly sensitive to thermal stress. Heat shock causes abrupt and dramatic loss of telomeric DNA in *ten1* plants, likely via deletional recombination. Second, we show that AtTEN1 has the properties of a heat-shock induced molecular chaperone. At elevated temperature, AtTEN1 rapidly assembles into high molecular weight homo-oligomeric complexes that efficiently suppress heat-induced aggregation of model protein substrates in vitro. Finally, we report that AtTEN1 specifically protects CTC1 from heat-induced aggregation in vitro, and from heat-induced protein degradation and loss of telomere association in vivo. Collectively, these observations define Arabidopsis TEN1 as a highly dynamic protein that works in concert with CTC1 to preserve telomere integrity in response to environmental stress.

INTRODUCTION

Telomeres are among the most highly dynamic structures in the genome. They form a platform for terminus binding proteins (termed shelterin in vertebrates) (de Lange, 2005) that sequester chromosome ends, protecting them from eliciting a DNA damage response. Telomere proteins also present the chromosome terminus as a substrate for replicative enzymes. Telomeric DNA consists of tandem arrays of G-rich repeats that terminate in a single-stranded 3′ overhang (G-overhang). During much of the cell cycle, the G-overhang is proposed to be concealed in a t-loop, wherein the single-strand terminus invades the telomeric duplex to form a Holliday junction-like structure (Griffith et al., 1999) inaccessible to telomerase (Smogorzewska et al., 2000). Failure to stabilize t-loops leads to the abrupt loss of telomeric DNA via recombinational deletion in a process termed telomere rapid deletion (TRD) (Lustig, 2003; Wang et al., 2004). TRD must be contained to avert catastrophic telomere shortening and replicative senescence. Telomere length homeostasis is achieved by a highly orchestrated, but poorly understood, series of conformational changes that sequentially convert the G-overhang into telomerase-extendable and nonextendable states (Blackburn, 2001; Teixeira et al., 2004). This binary switch is controlled by long-range protein interactions (Loayza and De Lange, 2003; Marcand et al., 1997), dynamic shifts among core components of telomere complexes (Jun et al., 2013), and posttranslational modification (Garg et al., 2014; Liu et al., 2014; Miyagawa et al., 2014; Zhang et al., 2013).

One telomere protein complex under intensive scrutiny is CST (Cdc13/CTC1, Stn1, Ten1). CST bears structural similarity to replication protein A (Gao et al., 2007; Sun et al., 2009) and associates with the G-overhang via an oligosaccharide-oligonucleotide binding fold (OB-fold) within the Cdc13/CTC1 subunit (Mitton-Fry et al., 2004). Stn1 and Ten1 each harbor single OB-fold domains and form a stable heterodimer (Petreaca et al., 2006). Mutation of budding yeast CST components causes degradation of the telomeric C-strand and hence increased length of the G-strand (Garvik et al., 1995; Grandin et al., 1997, 2001), phenotypes attributed to defects in telomeric DNA replication as well as chromosome end protection (Nugent et al., 1996; Xu et al., 2009). Cdc13 coordinates telomeric DNA replication by first facilitating G-strand synthesis through interactions with telomerase and then C-strand synthesis via association with DNA polymerase α/primase (Qi and Zakian, 2000). Unlike yeast CST, which stably and sequentially engages telomerase and DNA pol-α, vertebrate CST only transiently associates with telomeres, where it represses telomerase repeat addition processivity and stimulates Pol-α to facilitate the switch from G-strand to C-strand synthesis (Chen et al., 2012a; Lue et al., 2014). Vertebrate CST is also implicated in restoring replication fork progression following replication stress (Kasbek et al., 2013; Wang et al., 2012).

The prevailing view has been that CST functions as a trimeric complex, but mounting evidence indicates that subcomplexes of CST and individual subunits dynamically interact with each other and in some cases exchange for telomerase subunits and the conventional DNA replication machinery to promote telomere stability (Chen et al., 2012a; Grossi et al., 2004; Qi and Zakian, 2000). For example, yeast Stn1 inhibits telomerase binding to Cdc13 (Chandra et al., 2001), arguing that CST components must be modified in some fashion for replication, perhaps via

[1] Current address: National Institute of Ecology, 1210 Geumgang-ro, Maseo-myeon, Soecheon-gun 33657, Republic of Korea.
[2] Address correspondence to dshippen@tamu.edu.
The author responsible for distribution of materials integral to the findings presented in this article in accordance with the policy described in the Instructions for Authors (www.plantcell.org) is: Dorothy E. Shippen (dshippen@tamu.edu).
www.plantcell.org/cgi/doi/10.1105/tpc.16.00408

phosphorylation of Cdc13 (Li et al., 2009) and Stn1 (Liu et al., 2014). In some genetic backgrounds, STN1 and TEN1 stabilize chromosome ends in a Cdc13-independent manner (Holstein et al., 2014; Petreaca et al., 2006). Moreover, relative to human cells deficient in STN1 or CTC1, cells lacking TEN1 exhibit more severe growth defects, a higher frequency of chromosomes lacking telomeric DNA, and more anaphase bridges (Kasbek et al., 2013).

Data from *Arabidopsis thaliana* also support the conclusion that TEN1 makes unique contributions outside the context of the CST heterotrimer. Like *stn1* and *ctc1* mutants (Song et al., 2008; Surovtseva et al., 2009), *ten1-3* mutants display dramatic telomere shortening, extended G-overhangs, and end-to-end chromosome fusions (Leehy et al., 2013). Telomere failure culminates in defective stem cell proliferation and sterility (Hashimura and Ueguchi, 2011; Leehy et al., 2013). However, *ten1-3* mutants suffer even more genome instability than *stn1* or *ctc1* mutants (Leehy et al., 2013; Song et al., 2008; Surovtseva et al., 2009). In addition, TEN1 associates with a significantly smaller fraction of Arabidopsis telomeres than CTC1 (Leehy et al., 2013; Surovtseva et al., 2009), suggesting that TEN1 only transiently engages the chromosome terminus. Unlike STN1 and CTC1, which physically associate with enzymatically active telomerase in Arabidopsis, TEN1 negatively regulates telomerase repeat addition processivity (Leehy et al., 2013) and is not associated with active telomerase (Renfrew et al., 2014). In addition, AtTEN1 competes with POT1a, a positive regulator of telomerase processivity, for interaction with STN1; binding of TEN1 and POT1a by STN1 is mutually exclusive (Renfrew et al., 2014). Consequently, STN1 is proposed to dynamically exchange TEN1 for POT1a when telomerase extends Arabidopsis telomeres (Renfrew et al., 2014; Surovtseva et al., 2007).

Here, we report several unanticipated properties of AtTEN1 that reveal its remarkably dynamic nature. We demonstrate that TEN1, but not STN1, protects Arabidopsis telomeres from thermal stress-induced rapid telomere shortening in vivo. We provide evidence that AtTEN1 responds to heat stress by assembling into high molecular weight complexes with protein chaperone activity. Finally, we show that TEN1 has the capacity to protect CTC1 from heat-induced degradation in vivo. These findings provide new insight into AtTEN1 function and interactions and suggest that this protein plays a novel role in the plant response to the environment.

RESULTS

AtTEN1 and AtCTC1 Protect against Heat-Induced Telomere Truncation

To extend our analysis of Arabidopsis CST components, we employed the AtGenExpress Visualization Tool to examine RNA expression profiles under various abiotic stimuli (Supplemental Table 1; Kilian et al., 2007). The data indicated that heat shock, cold shock, and oxidative stress trigger a prompt increase in *AtTEN1* transcripts. Notably, this response is specific for *TEN1* as *CTC1*, *STN1*, and other telomere-related transcripts are largely unaffected. Among the abiotic stressors tested, heat shock had the greatest impact on *TEN1* expression. *AtTEN1* mRNA increased 2.3-fold after 3 h at 38°C, then returned to the basal level when plants were transferred to 25°C. By comparison, mRNAs in the Hsp70 family are elevated by 2- to 13-fold under the same conditions. This observation prompted us to investigate whether TEN1 might play a role in the plant response to thermal stress. Specifically, we asked if heat shock induced a change in telomere structure or integrity in *ten1-3* plants. *ten1-3* is not a null allele, but this mutation destabilizes TEN1 protein in vivo and abolishes STN1 binding in vitro (Leehy et al., 2013). Two week-old wild-type and *ten1-3* seedlings were placed at 42°C for 1 h and then returned to 23°C to recover. Plant samples were pooled to obtain sufficient material for analysis, and telomere length was assessed by primer extension telomere repeat amplification (PETRA). This PCR-based method assesses telomere length on individual chromosome arms (Heacock et al., 2004). Unlike the telomeres of wild-type seedlings, which range from 2 to 5 kb, *ten1-3* telomeres are more heterogeneous and on average 1 to 2 kb shorter (Leehy et al., 2013) (Figure 1A). Immediately following heat shock, telomere length was unchanged in *ten1-3* mutants, but during the 18-h recovery period, telomere tracts became more homogenous and shortened by an additional 1.5 to 2 kb, with most telomeres accumulating at the bottom end of the size range (Figure 1A). This result was not unique to a single telomere tract (Figure 1D; Supplemental Figure 1A). Furthermore, heat-induced telomere shortening was detected in plants deficient in CTC1, but not STN1 (Figures 1B and 1C; Supplemental Figures 1B and 1C). We conclude that TEN1 and CTC1, but not STN1, are needed to stabilize Arabidopsis telomeres in response to heat shock.

A time-course experiment showed that heat-induced telomere shortening occurred very rapidly in *ten1-3* mutants. One hour after heat shock, a broader size distribution of telomeres was observed (Figure 1D; Supplemental Figure 1D). After 3 h, only a faint signal could be detected in the range of untreated telomeres; the majority of telomeres were shorter than the shortest telomeres in untreated *ten1-3*. By 18 h, telomere appeared to be stabilized at the shorter length set point (Figure 1D).

We performed a quantitative telomere repeat amplification protocol to measure telomerase activity following heat shock. Previously we showed that telomerase activity is elevated in *ten1-3* flowers, reflecting an increase in repeat addition processivity (Leehy et al., 2013). In contrast, telomerase activity was not substantially different in *ten1-3* seedlings compared with the wild type (Supplemental Figure 1E), suggesting that TEN1-mediated control of telomerase is developmentally regulated. Heat stress reduced telomerase activity slightly in both the wild type and *ten1-3* mutants. Enzyme activity levels rebounded 18 h after treatment in the wild type, increasing 3-fold relative to untreated samples (Supplemental Figure 1E). This rebound effect was not observed *ten1-3* seedlings, and telomerase levels declined further to 4.5-fold the level of untreated *ten1-3* mutants. Why *ten1-3* mutants fail to exhibit this rebound effect for telomerase is unknown. Nevertheless, the data indicate that the abrupt heat-induced telomere shortening in *ten1-3* seedlings is not due to abrogation of telomerase activity.

AtTEN1 Exhibits Chaperone Activity on Model Protein Substrates

PSIPRED and FoldIndex indicated that AtTEN1 forms a single oligosaccharide binding fold with a disordered C terminus (Supplemental Figure 2A) (Leehy et al., 2013; McGuffin et al., 2000;

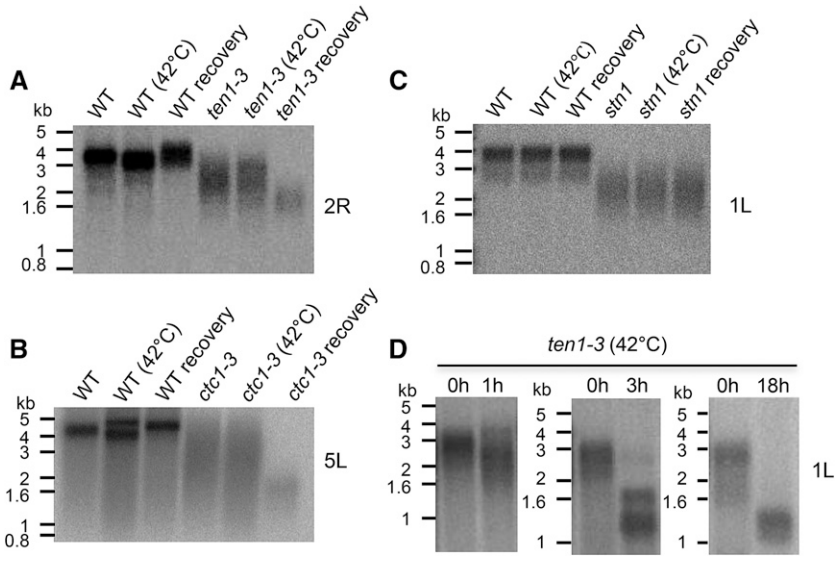

Figure 1. Plants Lacking AtTEN1 or AtCTC1 Undergo Rapid Telomere Shortening upon Heat Shock.

PETRA was used to measure telomere length of specific chromosome arms following heat shock. Wild-type and mutant plants were subjected to 42°C for 1 h and then returned to 23°C to recover. PETRA results for *ten1-3* (**[A]** and **[D]**), *ctc1-3* **(B)**, and *stn1-1* mutants **(C)** are shown. The telomere monitored right arm of chromosome 2 (2R), left arm of chromosome 5 (5L), or left arm of chromosome 1 (1L) are indicated. Blots were hybridized with labeled $(TTTAGGG)_5$. PETRA time-course analysis of *ten1-3* telomere length upon heat shock **(D)**. Representative results of at least three independent experiments are shown.

Prilusky et al., 2005). Notably, STN1 and TEN1 orthologs from yeast and vertebrates are not predicted to contain a similar unstructured domain. Since disordered and homo-oligomeric structures as well as thermo-sensitive phenotypes are characteristic of protein chaperones (Jang et al., 2004; Tompa and Csermely, 2004), we asked if AtTEN1 could act as a molecular chaperone. Recombinant AtTEN1 protein was expressed in *Escherichia coli* and purified to homogeneity as determined by mass spectrometry (Figure 2A; Supplemental Figure 2B). Analysis by SDS-PAGE revealed a single band of 16 kD, the expected molecular weight of a monomer (Figure 2A). In contrast, native-PAGE and size exclusion chromatography (SEC) revealed a discrete high molecular weight (HMW) complex of ~160 kD (Figures 2B and 2C). Immunoblotting with an AtTEN1 antibody confirmed that this species was indeed TEN1 (see Figure 3C).

To assess chaperone activity, we asked whether AtTEN1 could function as a "holdase" chaperone by protecting the model protein substrates malate dehydrogenase (MDH) and citrate synthase (CS) from heat-induced aggregation at 43°C as measured by light scattering (Jang et al., 2004). Incubation of the substrates with increasing amounts of chaperone protein prevents thermal aggregation, which is measured by monitoring turbidity. In the absence of ATP, TEN1 efficiently suppressed thermal aggregation of MDH and CS at a 1:1 molar ratio of substrate to TEN1 (Figure 2D; Supplemental Figure 3). In contrast, denatured TEN1 was unable to stabilize the model substrates. More importantly, STN1 did not prevent protein aggregation even in a 5-fold molar excess over substrate (Figure 2D; Supplemental Figure 3), indicating that the thermal stability afforded by TEN1 is a specific property of this protein. To verify the chaperone activity of AtTEN1, we compared the activities of AtTEN1 with the well-known chaperone proteins AtTDX and cPrxI. AtTDX is a plant-specific thioredoxin (Trx)-like redox protein that functions as both a disulfide reductase and a chaperone (Lee et al., 2009). cPrxI is from yeast and is categorized as a cytosolic 2-cysteine peroxiredoxin. cPrxI serves as a highly efficient molecular chaperone and a peroxidase; the dual functions are mediated by structural changes in response to different redox states (Jang et al., 2004). We found that AtTEN1 chaperone activity was 1.5-fold higher than the AtTDX (Lee et al., 2009) and similar to the cPrxI (Jang et al., 2004). Thus, we conclude that AtTEN1 can function as a bona fide chaperone to stabilize denatured model protein substrates.

Heat Shock Promotes AtTEN1 Assembly into Higher Order Spherical Structures with Increasing Chaperone Activity

A well-conserved feature of molecular chaperones is their tendency to reversibly assemble into higher order oligomers (Haley et al., 1998; Hendrick and Hartl, 1993). Therefore, we asked if heat-dependent structural changes were associated with AtTEN1. Native-PAGE revealed a marked structural alteration in TEN1 30 min after heat shock at 43°C (Figure 3A). Consistent with native PAGE analysis, AtTEN1 exists predominantly as a HMW complex of ~160 kD when subjected to SEC (Figures 2C and 3B). Following heat shock, an extra peak appeared in the void fraction (F-I) (Figure 3B). Both F-I and F-II fractions were analyzed again by immunoblotting with AtTEN1 antibody after native-PAGE. Unlike the TEN1 complex in F-II, the new ultra-HMW fraction (F-I) did not enter a 10% native gel (Figure 3C, top). On SDS-PAGE both the HMW and ultra-HMW fractions resolved into a single band with

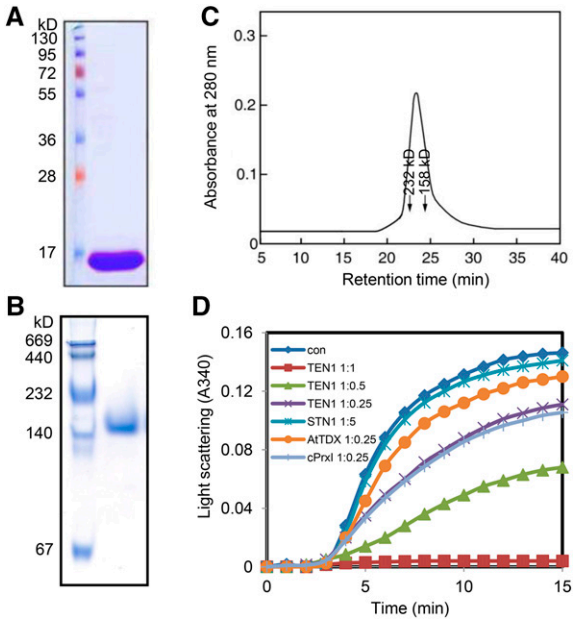

Figure 2. High Molecular Weight AtTEN1 Complexes and Chaperone Activity on a Model Protein Substrate.

(A) *E. coli* expressed AtTEN1 was resolved by 12% SDS-PAGE and stained with Coomassie blue.

(B) TEN1 HMW complexes were visualized by 10% native-PAGE. Molecular weight makers in kilodaltons are shown.

(C) Analysis of AtTEN1 by SEC. SEC was performed by FPLC using a Superdex 200 HR 10/30 column as described in the Methods. Catalase (232 kD) and aldolase (158 kD) markers are indicated.

(D) Chaperone activity was measured using 1.5 μM MDH as a substrate. Thermal aggregation of the substrate was examined in the presence of the proteins indicated. Reactions with AtTEN1 were conducted at molar ratios of substrate to AtTEN1 at 1:0.25, 1:0.5, and 1:1 at 43°C. Also shown are data for Arabidopsis thioredoxin-like chaperone (AtTDX), yeast peroxiredoxin (cPrxI), and a negative control reaction with only MDH substrate (con).

a molecular weight of 16 kD, corresponding to monomeric TEN1 (Figure 3C, bottom).

The fluorescence intensity of 1,1′-bi(4-anilino) naphthalene-5,5′-disulfonic acid (bis-ANS) binding to AtTEN1 was greater for the F-I fraction than the F-II fraction (Figure 3D), indicating that more hydrophobic patches on TEN1 are exposed by heat treatment in ultra-HMW complexes. Increased surface hydrophobicity correlates with increasing chaperone activities of proteins (Jang et al., 2004; Lee et al., 2009). As predicted, chaperone assays based on bis-ANS fluorescence revealed that the F-I fraction exhibited 3.5-fold higher activity than the F-II fraction (Figure 3E).

Cryo-electron microscopy was used to investigate the architecture of HMW AtTEN1 (Figure 3F). The protein concentration of F-I was insufficient for analysis and so F-II was examined. Analysis of 300 particles revealed four distinct size classes ranging from 9 to 13 nm in diameter (Figure 3F). The 2D architecture of the TEN1 particles is remarkably similar to the small heat shock-related αβ-crystallin chaperones from vertebrates (Braun et al., 2011), which like AtTEN1 assemble into a heterogeneous array of globular structures in response thermal stress. Taken together, these data indicate that the chaperone activity of AtTEN1 is associated with its ability to assume discrete higher order oligomeric structures.

Arabidopsis TEN1 Protects CTC1 from Thermal-Induced Aggregation in Vitro and Protein Degradation in Vivo

Since AtTEN1 has protein chaperone activity, we asked if it could stabilize CTC1. We previously reported robust interactions between Arabidopsis TEN1 and STN1 (Leehy et al., 2013) and STN1 with CTC1 (Surovtseva et al., 2009). A weak interaction between AtTEN1 and AtCTC1 was observed by in vitro coimmunoprecipitation (co-IP) (Figure 4A) and yeast two-hybrid analysis (Figure 4B), consistent with previous studies showing a weak interaction between yeast Ten1 and Cdc13 (Grandin et al., 2001).

We were unable to express full-length AtCTC1 in *E. coli.* Therefore, we generated two constructs that covered the amino (CTC1 N-term; 1 to 384 amino acids) and carboxy (CTC1 C-term; 385 to 1272 amino acids) regions of the protein. MDH and the two CTC1 constructs were expressed in *E. coli* and subjected to heat denaturation with or without AtTEN1. MDH and CTC1 were soluble at room temperature (RT), but following heat shock most of the MDH and CTC1 C-term became insoluble (Figures 4C and 4D). In contrast, CTC1 N-term was heat stable (Figure 4C). Addition of AtTEN1 at a molar ratio of 1:1 relative to substrate protected both MDH and CTC1 C-term from aggregation. When the ratio of substrate to AtTEN1 was reduced to 1:0.25, CTC1 C-term was solubilized, but not MDH, arguing that AtCTC1 is preferentially protected by AtTEN1 (Figure 4C). To test if heat stabilization of CTC1 simply reflected an interaction with a binding partner, we asked if AtSTN1 could stabilize the CTC1 C-term since the binding site for AtSTN1 lies within this region (Surovtseva et al., 2009). In marked contrast to AtTEN1, AtSTN1 failed to prevent CTC1 C-term aggregation even at a 1:1 molar ratio of AtSTN1 to CTC1 C-term (Figure 4D). This result is consistent with results from our chaperone activity assays for AtTEN1 and AtSTN1 on model protein substrates. Taken together, these findings provide additional support for a thermal protection function for AtTEN1, and not AtSTN1. The results also argue that AtCTC1 is a specific in vitro substrate for AtTEN1 activity.

We next asked if AtTEN1 stabilizes CTC1 in vivo. Immunoblotting with an AtCTC1 antibody detected two very diffuse bands in wild-type plants (Figure 5A; Supplemental Figure 4B). The upper bands ranged in size from ~95 to 150 kD, encompassing full-length AtCTC1 (~142 kD). Two diffuse lower molecular weight bands of 55 and 75 kD were also visible, likely representing proteolytic AtCTC1 breakdown products (Figure 5A). A similar profile was observed in *stn1-1* and *ten1-3* mutants, although the 72-kD product was absent. As expected, CTC1 was not detected in *ctc1-3* mutants (Surovtseva et al., 2009) (Figure 5A), verifying the specificity of the AtCTC1 antibody.

In wild-type plants, thermal stress decreased the relative abundance of AtCTC1 breakdown products and increased the fraction of full-length CTC1 (Figure 5A). The same result was observed in *stn1* mutants, demonstrating that AtSTN1 is not required for AtCTC1 stability in vivo. In marked contrast, no

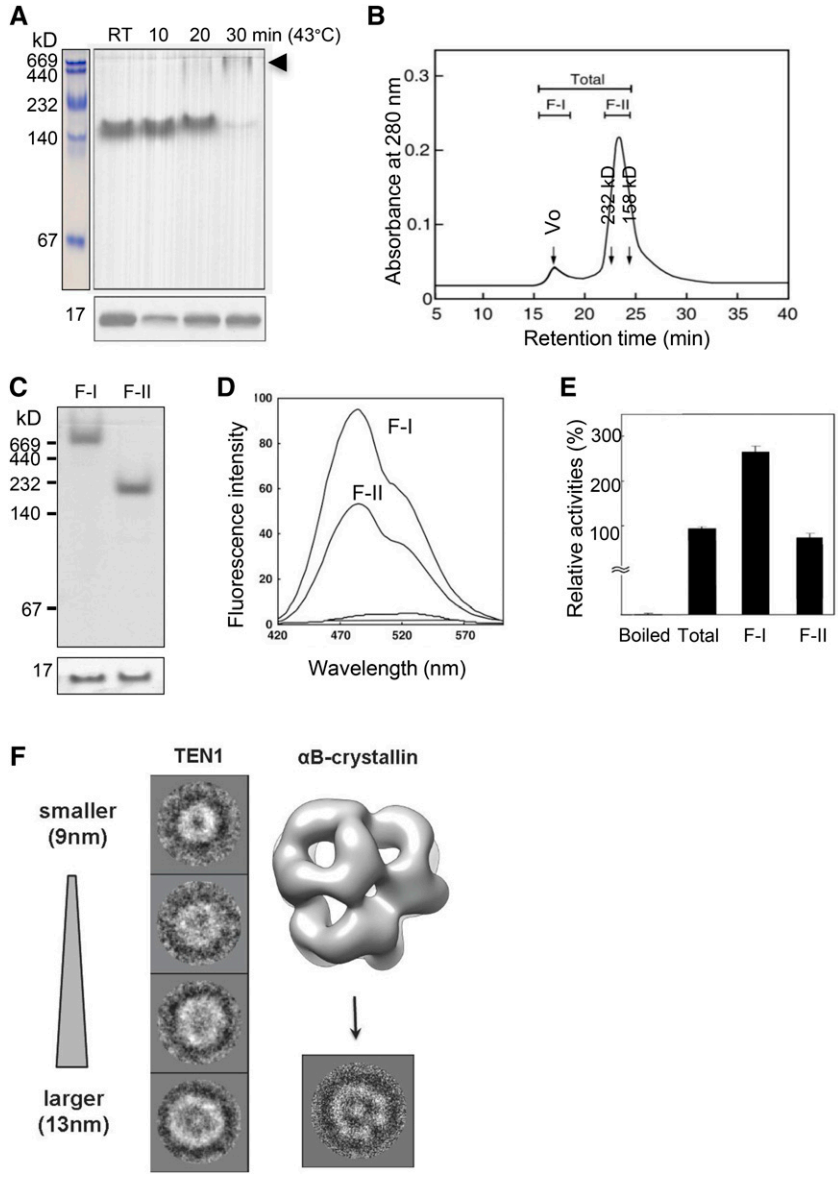

Figure 3. AtTEN1 Assumes Higher Order Oligomeric Structures.

The oligomeric status of AtTEN1 was analyzed by chromatographic, electrophoretic, and cryo-EM techniques.
(A) AtTEN1 was subjected to heat treatment at 43°C for the times indicated followed by immunoblotting with AtTEN1 antibody after separating the protein by 10% native (top) or SDS-PAGE (bottom).
(B) SEC was performed on heat-treated protein for 20 min as in **(A)**. Molecular weight standards are indicated. Purified proteins were divided and collected into two fractions (F-I and F-II).
(C) The F-I and F-II fractions were concentrated and subjected to immunoblotting with AtTEN1 antibody after resolution by 10% native or SDS-PAGE.
(D) F-I and F-II fractions were concentrated, and changes in TEN1 hydrophobicity were measured using a bis-ANS probe, which binds to hydrophobic clusters of aminoacyl residues.
(E) Relative activity of chaperone function was analyzed based on bis-ANS fluorescence. The activities of SEC fractions were compared with total protein, whose activity was set to 100%. Denatured (boiled) AtTEN1 protein was included as a negative control. Data represent means of at least three independent experiments.
(F) 2D class averages of cryo-EM data for TEN1 F-II complexes are indicated with a representative of each class. The fractions of molecules in each class are 26, 27, 23, and 24%, from top to bottom. The size of each class average is 21 × 21 nm. The 2D class average of the 13-nm-diameter TEN1 oligomer shows features similar to the αB-crystallin image. A 2D projection of the αB-crystallin generated from its density map obtained from the EM databank (accession ID: EMD 1776) is shown in the right column. The projection image of αB-crystallin is 25 × 25 nm.

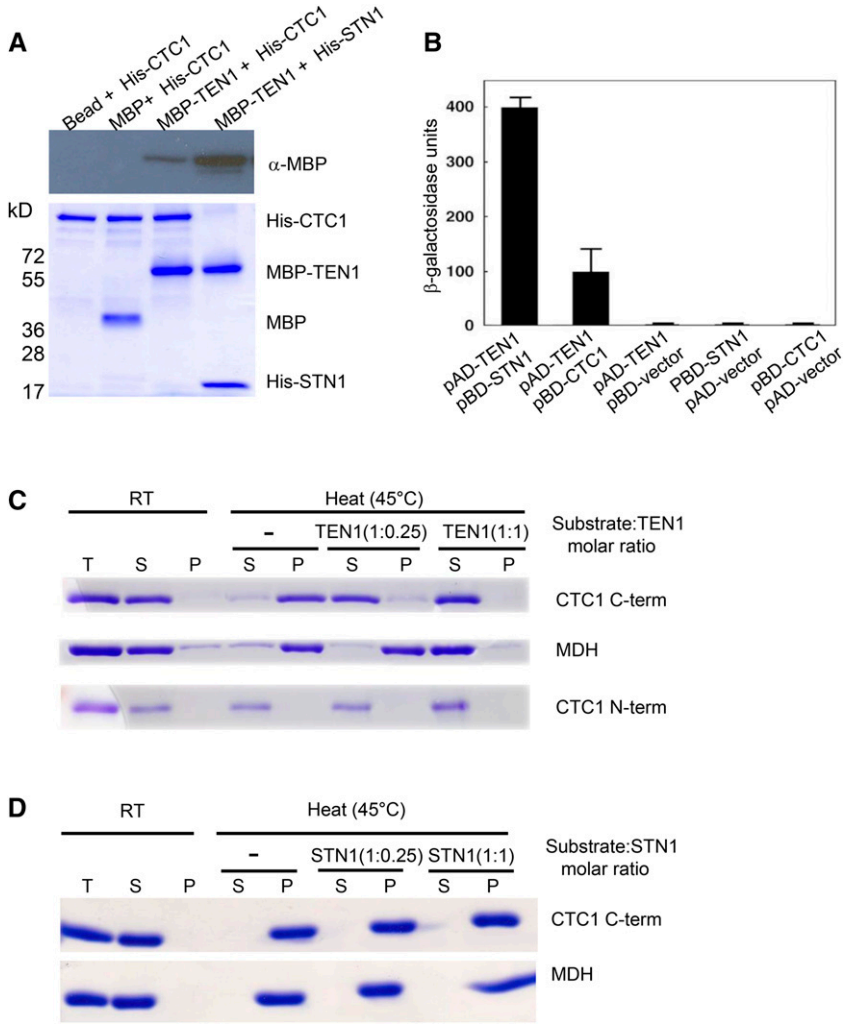

Figure 4. AtTEN1 Protects CTC1 from Thermal-Induced Aggregation in Vitro.

(A) Co-IP immunoblot data with recombinant MBP-fusion CST proteins and His-tagged CST proteins are shown. Immunoprecipitation of MBP-fusion TEN1 using His tagged CTC1 and STN1 recombinant proteins by anti-His antibody conjugated agarose beads. Co-IP protein input controls with same amounts included (lower panel).

(B) Results of yeast two-hybrid assays for CST interactions. Numbers indicate arbitrary units to show relative activities of protein-protein interactions using *o*-nitrophenyl-D-galactoside activity. pAD and pBD denote an activation domain or a binding domain containing vector. TEN1, STN1, and CTC1 with empty vectors are included as controls for self-activation. Values represent means of at least three independent experiments.

(C) and **(D)** In vitro protection assay.

(C) AtTEN1 protects AtCTC1 from heat-induced aggregation. CTC1 N-term (1 to 384 amino acids), CTC1 C-term (385 to 1272 amino acids), and MDH were incubated at RT and 45°C for 30 min with or without AtTEN1.

(D) AtSTN1 does not protect CTC1 from heat-induced aggregation. CTC1 C-term (385 to 1272 amino acids) and MDH were incubated at RT and 45°C for 30 min with or without STN1. For **(C)** and **(D)**, equal amounts of total protein (T) were centrifuged and divided into soluble (S; stable) or pellet (P; unstable) fractions. Proteins were resolved by SDS-PAGE followed by Coomassie blue staining.

full-length AtCTC1 was detected in *ten1-3* mutants upon heat shock, only a series of bands ranging from ~100 to 55 kD. Conversely, in a *ten1-3* genetic complementation line where ectopic expression of AtTEN1 protein is ~2-fold higher than AtTEN1 in wild-type plants (Leehy et al., 2013), full-length CTC1 was stabilized and the 55-kD breakdown product decreased. These observations indicate that CTC1 is protected from thermal-induced degradation by TEN1 in vivo.

We next assessed the oligomeric status of endogenous AtTEN1 after thermal stress. In the absence of heat shock, AtTEN1 migrated as a discrete band between 232 and 140 kD on native PAGE (Figure 5B). Because human and yeast CST complexes exhibit an apparent molecular weight of ≥500 kD in SEC (Lue et al., 2013; Miyake et al., 2009), we suspect this AtTEN1-containing complex does not represent a trimeric Arabidopsis CST. Strikingly, under the same heat shock conditions that destabilized AtCTC1,

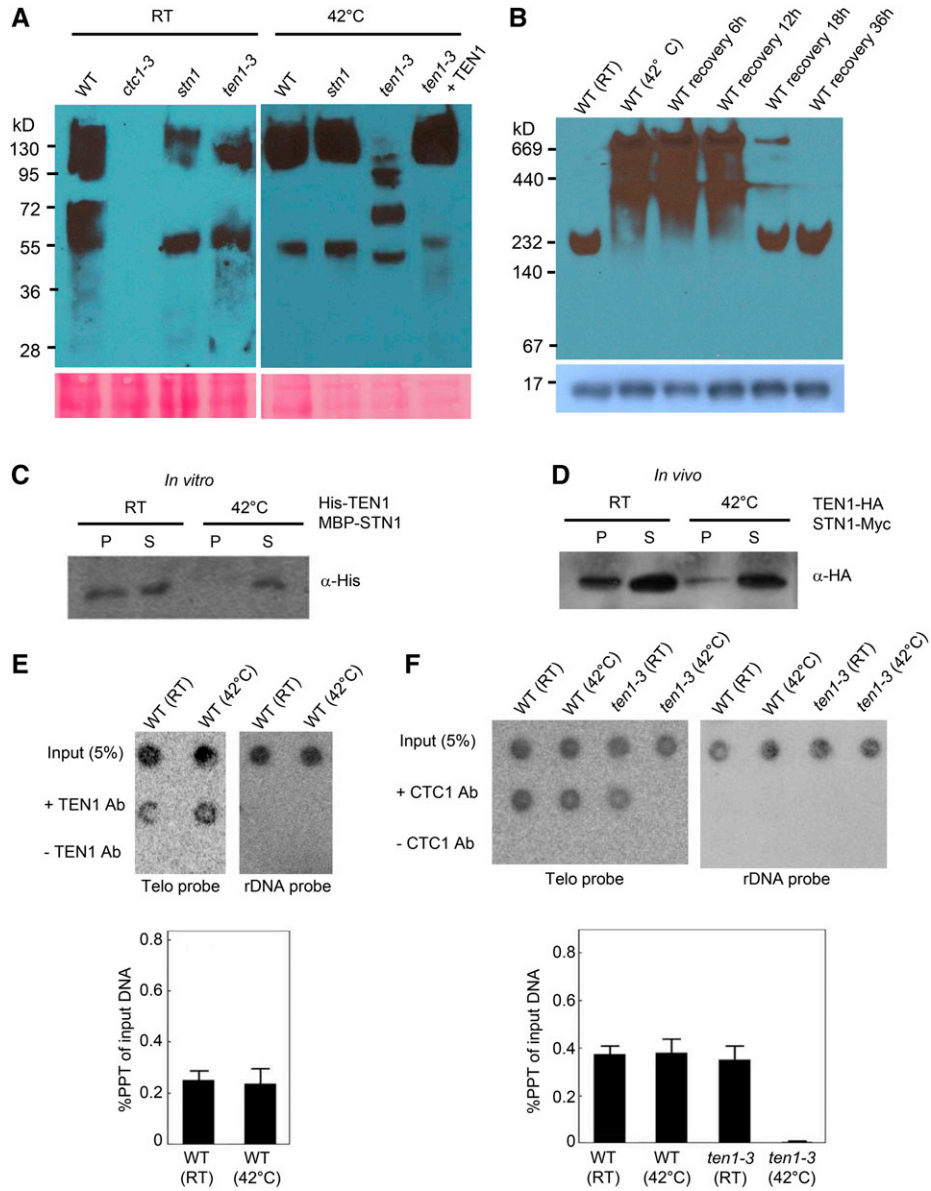

Figure 5. AtTEN1 Promotes CTC1 Stability and Telomere Association following Heat Shock.

(A) Heat stress destabilizes AtCTC1 in vivo. The wild type, *stn1*, *ten1-3*, and an AtTEN1 complementation line of *ten1-3* mutant plants were incubated at RT or at 42°C for 30 min. Equal amounts of total protein were resolved by SDS-PAGE followed by immunoblotting with AtCTC1 antibody. An image of the *Ponceau S*-stained membrane is shown in the bottom panel.

(B) AtTEN1 assembles into higher molecular weight oligomers in response to heat shock. Immunoblot analysis of AtTEN1 was performed on total protein isolated from plants kept at RT or subjected to heat shock at 42°C for 30 min. Extracted protein was resolved by 10% native-PAGE.

(C) and **(D)** Temperature-dependent interaction of AtTEN1 with STN1 in vitro.

(C) Results of co-IP assays performed with *E. coli* expressed His-TEN1 and MBP-STN1 in the presence or absence of heat treatment. IP was performed with anti-MBP antibody followed by immunoblotting with anti-His antibody. S, supernatant; P, pellet.

(D) AtTEN1-HA and AtSTN1-Myc were transiently expressed in tobacco leaves and TEN1 was pulled down by with anti-Myc. The immunoblot was probed with anti-HA antibody.

(E) and **(F)** Telomeric DNA association of AtCTC1 and AtTEN1. ChIP was performed on the wild type and *ten1-3* mutants treated or untreated with heat shock using anti-TEN1 antibody **(E)** and anti-CTC1 antibody **(F)** followed by dot blot analysis with a [^{32}P] 5′ end-labeled $(T_3AG_3)_5$ oligonucleotide probe. A [^{32}P] 5′ end-labeled rDNA (18S+5S) was used as a control probe. Quantification of TEN1 and CTC1 telomere ChIP data (lower panel). IP signal is represented as percent precipitation of input DNA. Error bars represent SE of the mean from three independent biological replicates.

AtTEN1 formed extremely diffuse ultra-HMW complexes ranging from 160 to at least 669 kD (Figure 5B). Eighteen hours after heat-treated seedlings were restored to 23°C, the ultra HMW complexes diminished significantly, and by 36 h, AtTEN1 returned to its pre-heat shock size (Figure 5B). SDS-PAGE indicated that the steady state level of AtTEN1 was essentially unchanged throughout the time course (Figure 5B, bottom). Whether the lower molecular weight AtTEN1 complexes that accumulated during the recovery period represent disassembled ultra-HMW complexes or new AtTEN1 synthesis is unknown.

In conjunction with formation of ultra HMW AtTEN1 complexes, heat shock disrupted AtTEN1 binding to AtSTN1 in vitro (Figure 5C) and in vivo as shown by a heat denaturation experiment performed with *Nicotiana benthamiana* leaves transiently expressing AtTEN1 and AtSTN1 (Figure 5D). These results indicate that thermal stress triggers a major conformational shift in AtTEN1, which is coincident with decreased binding to AtSTN1, increased chaperone activity, and AtCTC1 stabilization.

Arabidopsis TEN1 Stabilizes the Association of CTC1 with Telomeres following Heat Shock

Since heat shock causes AtTEN1 to assemble into ultra HMW oligomers, we asked if telomere-bound AtTEN1 increases under these conditions. Chromatin immunoprecipitation (ChIP) revealed no significant difference in the level of telomere-associated AtTEN1 before or after heat shock (Figure 5E), suggesting that HMW TEN1 complexes do not accumulate at telomeres. Finally, we asked if the abrupt telomere shortening associated with heat stress in *ten1-3* mutants reflects the loss of CTC1 from telomeres. There was no difference in the telomere association of CTC1 in the wild type in the presence or absence of heat shock (Figure 5F). In addition, the level of telomere-bound CTC1 in *ten1-3* mutants was similar to the wild type at room temperature, indicating that TEN1 is not required for CTC1 localization at chromosome ends. In contrast, CTC1 binding to telomeric DNA was completely abolished when *ten1-3* plants were subjected to heat shock (Figure 5F). We conclude that AtTEN1 stabilizes telomere-bound AtCTC1 under heat stress to promote telomere integrity.

DISCUSSION

The telomere is a remarkably dynamic region of the genome that fluctuates in each cell cycle from a sequestered, fully protected state to an open conformation accessible to the replication machinery. The molecular basis for these conformational switches is largely unknown. In this study, we provide evidence that a core constituent of the CST complex is itself a highly dynamic protein with molecular chaperone activity.

Chaperone Activity of AtTEN1

Our results show that AtTEN1 has the biochemical, biophysical, and structural properties of a small heat shock-like protein chaperone. AtTEN1 prevents thermal aggregation of model protein substrates in vitro with activity that is robust and comparable to other antiaggregation chaperones. As is typical for small heat shock chaperones (Haslbeck et al., 2005; Hendrick and Hartl, 1993; Sun and MacRae, 2005), thermal stress triggers an increase in AtTEN1 hydrophobicity and elevates its chaperone activity. In addition, the heat-induced biochemical changes within AtTEN1 are accompanied by a large conformational shift, resulting in AtTEN1 dissociation from AtSTN1 and assembly into ultra-HMW homo-oligomeric spheres. In contrast to the archetypal small heat shock proteins that form homogeneous globular structures consisting of either 12 or 24 subunits (Haslbeck et al., 2005), our cryo-electron microscopy (cryo-EM) data indicate that HMW TEN1 oligomers more closely resemble αβ-crystallins of the vertebrate eye lens (Braun et al., 2011). In response to heat shock, αβ-crystallins assemble into a heterogeneous population of spherical frameworks ranging in size from 6- or 12-mers to 24- or 48-mers (Braun et al., 2011; Peschek et al., 2013). Both conventional sHsps and αβ-crystallin harbor a large internal cavity (Haslbeck et al., 2005; Peschek et al., 2009; Raman and Rao, 1997), which also may be present in AtTEN1. It is possible that the larger AtTEN1 particles (13 nm) provide an interior scaffold to stabilize substrate proteins, while smaller AtTEN1 complexes represent assembly intermediates. 3D reconstruction analysis will be necessary to test this hypothesis.

Although canonical sHsps bind a wide range of target proteins, αβ-crystallins preferentially stabilize certain classes of substrates such as aquaporin 0 (AQP0) (Swamy-Mruthinti et al., 2013). AtTEN1 may also have preferential targets in vivo, one being AtCTC1. We found that AtTEN1 not only protects AtCTC1 from thermal-induced aggregation in vitro and protein degradation in vivo, but also is required to stabilize telomere-bound AtCTC1 in response to heat stress. In contrast, AtSTN1 fails to exhibit chaperone activity on model substrates and cannot protect AtCTC1 from thermal aggregation, indicating that AtTEN1-mediated protection of AtCTC1 is specific. Importantly, because AtSTN1 binds AtCTC1 with higher affinity than AtTEN1 (Chen et al., 2013; Miyake et al., 2009), the thermal stabilization of AtCTC1 by AtTEN1 is consistent with a catalytic chaperone activity rather than stabilization as a stoichiometric member of the CST complex.

A chaperone-related function for AtTEN1 is attractive given the central role of CST in coordinating the exchange of macromolecular DNA replication complexes on chromosome ends during S phase. While chaperones have previously been implicated in the assembly and disassembly of large telomere-related complexes (DeZwaan et al., 2009; Forsythe et al., 2001; Grandin and Charbonneau, 2001), the specificity of these interactions and their precise role in stimulating telomere maintenance are unclear. Our data define AtTEN1 as a multifunctional protein that forms a stable binary complex with AtSTN1, but in the presence of heat shock can dissociate from AtSTN1 and assemble into HMW homo-oligomers with chaperone activity. We note that the intrinsically disordered domain within AtTEN1 is predicted to encompass the STN1 binding interface, based on the yeast and human TEN1-STN1 crystal structures (Bryan et al., 2013; Sun et al., 2009). This observation can explain our failure to obtain AtTEN1 mutants that separate STN1 binding from homo-oligomerization: If the two outcomes are mutually exclusive, AtSTN1 binding could negatively regulate the chaperone activity of AtTEN1.

A Role for AtTEN1 in Controlling Telomere Dynamics

Figure 6 presents a speculative model for how dynamic interactions of AtTEN1 affect telomere maintenance and stability. We

previously showed that AtTEN1 is a negative regulator of telomerase (Leehy et al., 2013) and further that binding of TEN1 and the telomerase processivity factor POT1a with STN1 is mutually exclusive (Renfrew et al., 2014). Thus, exchange of AtTEN1 for POT1a could help to convert telomeres to a telomerase-accessible conformation (Figure 6A). After STN1 disengages, AtTEN1 is free to assemble into higher order complexes with chaperone activity. "Activated" AtTEN1 has the potential to stabilize different conformations of CTC1 to coordinate several protein exchanges. For example, once the telomeric G-strand is extended by telomerase, CTC1/STN1 must swap telomerase for DNA Pol-α to enable synthesis of the C-rich telomeric strand (Huang et al., 2012; Qi and Zakian, 2000). In addition, when telomere replication is complete, Pol-α must be dislodged to generate a fully protected, inaccessible chromosome terminus. We suspect that direct interactions of AtTEN1 with CTC1 are transient. We detected only weak binding between these proteins in vitro, and AtTEN1 occupancy at telomeres is significantly lower than CTC1 (Leehy et al., 2013; Surovtseva et al., 2009). Even after heat shock when TEN1 forms ultra-HMW oligomers, there is no substantial increase in telomere-bound TEN1. CST remains the best candidate for a chromosome capping complex in Arabidopsis, since functional shelterin orthologs have yet to be defined (Fulcher and Riha, 2016; Nelson and Shippen, 2012). Consequently, reestablishing the STN1-TEN1 interaction may be an integral part of terminating the telomere replication cycle and establishing a fully protected, telomerase inaccessible state (Figure 6A).

TEN1 as a Guardian for Telomere Integrity

In addition to a potential role in modulating telomere replication, our data indicate that TEN1 protects Arabidopsis telomeres from thermal stress by stabilizing CTC1 (Figure 6B). In the absence of TEN1, telomeres in Arabidopsis seedlings shorten abruptly and dramatically following heat shock. We considered the possibility that heat-induced telomere shortening was caused by depletion of telomerase activity. Although we observe a slight decrease in telomerase activity upon heat stress, *tert* mutants completely devoid of telomerase activity lose telomeric DNA at a rate of 250 to 500 bp across an entire plant generation (Riha et al., 2001), less DNA than is lost in the 18-h window following heat shock. An alternative explanation for abrupt telomere shortening is that heat stress induces replication fork stalling in the telomeric duplex region, which can trigger double-strand DNA breaks and loss of telomeric DNA (Baird, 2008). However, plants at this developmental stage undergo cell division on average only once every 18 h

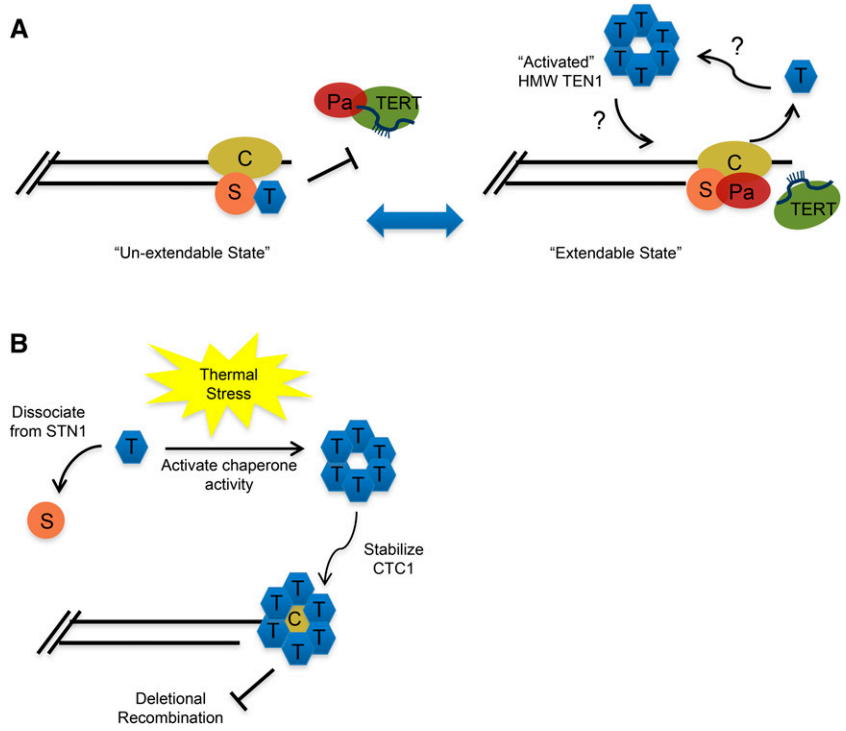

Figure 6. A Speculative Model for Dynamic Interactions of AtTEN1.

(A) AtTEN1 may play a role in regulating the switch of telomeres from the telomerase unextendable to the extendable state. The CST complex is proposed to form a protective cap for Arabidopsis telomeres. Unlike STN1 and CTC1, TEN1 is not associated with enzymatically active telomerase. Thus, the exchange of TEN1 for POT1a may help to convert telomere ends into a telomerase extendable state. Once dislodged from STN1, TEN1 is free to form "activated" higher order structures (illustrated for simplicity as a hexamer) with chaperone activity. Association of HMW TEN1 with CTC1 could facilitate conformational changes in CTC1 that promote the access of telomerase or DNA Pol-α to the chromosome end.
(B) In response to thermal stress, TEN1 is dislodged from STN1 and assembles into "activated" HMW complexes that stabilize CTC1 and protect telomeres from deletional recombination (TRD). C, CTC1; S, STN1; T, TEN1; Pa, POT1a.

(Beemster and Baskin, 1998); thus, replication fork stalling is unlikely to account for the precipitous loss of telomeric DNA. The most likely explanation for heat-induced telomere shortening is DNA processing by a nonreplicative recombination mechanism such as TRD.

How could thermal stress lead to TRD? Plant genomes are exquisitely responsive to environmental assault, and a variety of abiotic stressors, including radiation (Lebel et al., 1993), heavy metals (Rahavi et al., 2011), and elevated temperature (Boyko et al., 2010), as well as biotic stresses in the form of pathogen attack (Kovalchuk et al., 2003) increase the frequency of homologous recombination (HR). Elevated HR can persist for multiple plant generations even after the stress is eliminated (Molinier et al., 2006). Whereas a high rate of HR increases the ability to adapt to adverse conditions, it may also stimulate TRD. Thus, a telomere-associated chaperone such as AtTEN1 would be a useful weapon for plants to avert TRD in a hostile environment. Studies in human cells support the conclusion that telomere protein complexes evolved multiple interconnected strategies to stabilize and actively restore the integrity of chromosome ends in response to environmental assault. Human telomeres, for example, are less susceptible to UV induced photo-adducts than bulk chromosomal DNA (Parikh et al., 2015). Further, the shelterin components POT1, TRF1, and TRF2 physically interact with and stimulate factors necessary for repair of oxidative and UV damage (Miller et al., 2012; Parikh et al., 2015). In Arabidopsis, both AtTEN1 protein and mRNA are rapidly responsive to temperature and perhaps other environmental stimuli. We hypothesize that the complex regulation of AtTEN1 and its chaperone function define a regulatory pathway linking telomere protein to environmental stress and genome stability in plants.

METHODS

Plant Materials, Growth Conditions, and Treatments

The *ctc1-3*, *stn1*, and *ten1-3* mutants were described previously (Leehy et al., 2013; Song et al., 2008; Surovtseva et al., 2009). *Arabidopsis thaliana* were grown at 23°C under long-day conditions (16 h light/8 h dark) on either 0.5× Murashige and Skoog plates or on Sunshine soil mix.

Plasmid Construction and Yeast Two-Hybrid Analysis

Arabidopsis TEN1 was PCR-amplified from an Arabidopsis cDNA library using *AtTEN1* F primer containing a *Bam*HI site and the initiation codon and with AtTEN1 R primer containing both an *Xho*I site and the stop codon, respectively. N- or C-terminal truncated *AtCTC1* constructs comprising amino acid residues 1 to 384 and 385 to 1272 were amplified from pET28a-AtCTC1 as a template. PCR products were subcloned into the pGEM-Teasy vector (Promega). Inserts were digested with *Bam*HI and *Xho*I, and ligated into the corresponding sites of pET-28a vector (Novagen) for expression in *Escherichia coli*. All of the constructs were verified by sequencing.

For yeast two-hybrid analysis, pBD-GAL4-AtTEN1, pAD-GAL4-AtSTN1, and pAD-GAL4-AtCTC1 were generated and yeast two-hybrid assays were performed using SD/-Leu/-Trp/-His/-Ade selection medium with 10 mM 3-aminotriazole. After transformation, positive clones were subjected to the *o*-nitrophenyl-D-galactoside assay for β-galactosidase activity in yeast to check binding strength as described (Clontech).

Purification of Recombinant TEN1 and CTC1

E. coli BL21(DE3) pLysS transformed with pET-28a encoding wild-type or mutant AtTEN1 and AtCTC1 proteins was cultured at 30°C in Luria-Bertani medium supplemented with kanamycin (50 μg/mL) until the OD of the culture at 600 nm reached 0.3. After additional incubation at 4°C for 30 min, 0.4 mM isopropyl-β-D-thiogalacto-pyranoside was added to the culture and incubated for 14 h at 16°C. Cells were harvested by centrifugation and stored at −70°C until use. Frozen cells were suspended in PBS buffer and disrupted by sonication. Soluble crude extract was loaded into a Ni-NTA column. Histidine-tagged protein was affinity-purified by Ni-NTA agarose. Purified AtTEN1 was dialyzed and used for biochemical analysis and for preparation of polyclonal antibody.

Protein Identification

Recombinant AtTEN1 protein was digested with trypsin and subjected to mass spectrometry analysis using MALDI-TOF-MS. All MALDI-TOF-MS spectra were searched against the NCBI protein database using the MASCOT search program (http://www.matrixscience.com).

SEC, Co-IP, and Yeast Two-Hybrid Assays

SEC on FPLC (Amersham Pharmacia) was performed with a Superdex 200 HR 10/30 column equilibrated at a flow rate of 0.5 mL/min at 25°C with 50 mM HEPES, pH 8.0, buffer containing 100 mM of NaCl. Protein peaks (A_{280}) were isolated and concentrated using a Centricon YM-10 (Millipore). Protein interactions of AtTEN1, AtSTN1, and AtCTC1 were tested using a co-IP assay (Leehy et al., 2013) and two-hybrid analysis (Lee et al., 2006).

Chaperone Assays and bis-ANS Fluorescence Measurements

Chaperone activity was measured using MDH and CS substrates as described (Jang et al., 2004; Lee et al., 2009). Porcine heart mitochondrial MDH, CS, DTT, and H_2O_2 were purchased from Sigma-Aldrich. Turbidity due to substrate aggregation was monitored in a DU800 spectrophotometer (Beckman) equipped with a thermostatic cell holder. F-I and F-II fractions of TEN1 taken in 50 mM HEPES buffer were incubated with 10 μM bis-ANS. Hydrophobic domain exposure of TEN1 was examined by measuring the binding of bis-ANS to each fraction with a FM25 spectrofluorometer (Kontron) as described (Jang et al., 2004). bis-ANS was from Molecular Probes.

Protein Stability Assays

AtCTC1 N-term, AtCTC1 C-term, and MDH were incubated at RT and 45°C for 30 min with or without recombinant AtTEN1 or AtSTN1. Heat-treated samples were centrifuged, and stable and unstable fractions were displayed on an SDS-PAGE gel. To monitor protein stability in vivo, 4-week-old seedlings from wild-type, *stn1*, *ten1-3*, and *ten1-3* complementation lines (Hashimura and Ueguchi, 2011) were incubated at RT or at 42°C for 30 min. Total protein was extracted and equal amounts (45 μg) were resolved by SDS-PAGE followed by immunoblotting with AtCTC1 antibody. The oligomeric status of TEN1 in wild-type Arabidopsis was assessed at RT and upon heat shock by immunoblotting of total protein with an AtTEN1-antibody (Leehy et al., 2013).

Cryo-EM and Image Processing

Following SEC, F-II fractions of AtTEN1 were frozen in vitreous ice on a Quantfoil R2/1 holey carbon grid with a FEI Vitrobot. Fifty cryo-EM images were acquired at an effective magnification of 81081× using a FEI TECNAI F20 cryo-electron microscope operated at 200 kV. A total of 300 particles was selected and particles were averaged into 16 reference-free class averages using EMAN2 (Tang et al., 2007). After careful screening, four classes of different particle sizes were compiled and shown in the figure.

Telomere Analysis

DNA was isolated using 2× CTAB as described previously (Leehy et al., 2013). The heat shock seedling sample was collected after heat treatment at 42°C for 1 h. To determine the length of specific telomere tracts, PETRA (Heacock et al., 2004) was performed with 2 μg of DNA. Quantitative telomere repeat amplification protocol was performed as previously described (Leehy et al., 2013). For telomere ChIP, 5 g of 2-week-old plant tissues was harvested after heat treatment and ChIP was performed as described (Saleh et al., 2008). Filter binding assays were performed using a [^{32}P] 5′ end-labeled $(T_3AG_3)_5$ oligonucleotide probe. A [^{32}P] 5′ end-labeled rDNA (18S+5S) was used as a control probe.

Accession Numbers

Sequence data from this article can be found in the Arabidopsis Genome Initiative or GenBank/EMBL databases under the following accession numbers: MDO1/TEN1 (AT1G56260), CTC1 (AT4G09680), and STN1 (AT1G07130).

Supplemental Data

Supplemental Figure 1. Heat-induced telomere shortening in *ten1-3* and *ctc1-3* mutants.

Supplemental Figure 2. Characterization of AtTEN1 protein.

Supplemental Figure 3. Chaperone activity of Arabidopsis TEN1 protein.

Supplemental Figure 4. Specificity of the CTC1 polyclonal antibody.

Supplemental Table 1. Transcriptome data for Arabidopsis telomere-related transcripts in response to abiotic stressors.

ACKNOWLEDGMENTS

We thank Carolyn Price and Hays Rye for thoughtful comments on the manuscript, the Microscopy and Imaging Center at Texas A&M University for providing instrumentation for the cryo-EM data collection, and the Texas A&M High Performance Research Computing Center for providing the computational resources for the data processing. This work was supported by the Next-Generation BioGreen Program (SSAC, Grant PJ01137901), RDA, Korea to S.Y.L., National Institutes of Health (R01-GM065383) to D.E.S., startup funding from the Department of Biochemistry and Biophysics at Texas A&M University and the Center for Phage Technology jointly sponsored by Texas AgriLife and Texas A&M University to J.Z., and Welch Foundation Grant A-1863 to J.Z.

AUTHOR CONTRIBUTIONS

J.R.L. and D.E.S. wrote the article. J.R.L. and D.E.S designed the research. J.R.L., J.Z., X.X., and S.Y.L. performed research and analyzed data.

Received May 25, 2016; revised August 25, 2016; accepted September 6, 2016; published September 8, 2016.

REFERENCES

Baird, D.M. (2008). Telomere dynamics in human cells. Biochimie **90:** 116–121.

Beemster, G.T., and Baskin, T.I. (1998). Analysis of cell division and elongation underlying the developmental acceleration of root growth in *Arabidopsis thaliana.* Plant Physiol. **116:** 1515–1526.

Blackburn, E.H. (2001). Switching and signaling at the telomere. Cell **106:** 661–673.

Boyko, A., Blevins, T., Yao, Y., Golubov, A., Bilichak, A., Ilnytskyy, Y., Hollunder, J., Meins, F., Jr., and Kovalchuk, I. (2010). Transgenerational adaptation of Arabidopsis to stress requires DNA methylation and the function of Dicer-like proteins. PLoS One **5:** e9514.

Braun, N., Zacharias, M., Peschek, J., Kastenmüller, A., Zou, J., Hanzlik, M., Haslbeck, M., Rappsilber, J., Buchner, J., and Weinkauf, S. (2011). Multiple molecular architectures of the eye lens chaperone αB-crystallin elucidated by a triple hybrid approach. Proc. Natl. Acad. Sci. USA **108:** 20491–20496.

Bryan, C., Rice, C., Harkisheimer, M., Schultz, D.C., and Skordalakes, E. (2013). Structure of the human telomeric Stn1-Ten1 capping complex. PLoS One **8:** e66756.

Chandra, A., Hughes, T.R., Nugent, C.I., and Lundblad, V. (2001). Cdc13 both positively and negatively regulates telomere replication. Genes Dev. **15:** 404–414.

Chen, L.Y., Majerská, J., and Lingner, J. (2013). Molecular basis of telomere syndrome caused by CTC1 mutations. Genes Dev. **27:** 2099–2108.

Chen, L.Y., Redon, S., and Lingner, J. (2012a). The human CST complex is a terminator of telomerase activity. Nature **488:** 540–544.

de Lange, T. (2005). Shelterin: the protein complex that shapes and safeguards human telomeres. Genes Dev. **19:** 2100–2110.

DeZwaan, D.C., Toogun, O.A., Echtenkamp, F.J., and Freeman, B.C. (2009). The Hsp82 molecular chaperone promotes a switch between unextendable and extendable telomere states. Nat. Struct. Mol. Biol. **16:** 711–716.

Forsythe, H.L., Jarvis, J.L., Turner, J.W., Elmore, L.W., and Holt, S.E. (2001). Stable association of hsp90 and p23, but Not hsp70, with active human telomerase. J. Biol. Chem. **276:** 15571–15574.

Fulcher, N., and Riha, K. (2016). Using centromere mediated genome elimination to elucidate the functional redundancy of candidate telomere binding proteins in *Arabidopsis thaliana.* Front. Genet. **6:** 349.

Gao, H., Cervantes, R.B., Mandell, E.K., Otero, J.H., and Lundblad, V. (2007). RPA-like proteins mediate yeast telomere function. Nat. Struct. Mol. Biol. **14:** 208–214.

Garg, M., Gurung, R.L., Mansoubi, S., Ahmed, J.O., Davé, A., Watts, F.Z., and Bianchi, A. (2014). Tpz1TPP1 SUMOylation reveals evolutionary conservation of SUMO-dependent Stn1 telomere association. EMBO Rep. **15:** 871–877.

Garvik, B., Carson, M., and Hartwell, L. (1995). Single-stranded DNA arising at telomeres in cdc13 mutants may constitute a specific signal for the RAD9 checkpoint. Mol. Cell. Biol. **15:** 6128–6138.

Grandin, N., and Charbonneau, M. (2001). Hsp90 levels affect telomere length in yeast. Mol. Genet. Genomics **265:** 126–134.

Grandin, N., Damon, C., and Charbonneau, M. (2001). Ten1 functions in telomere end protection and length regulation in association with Stn1 and Cdc13. EMBO J. **20:** 1173–1183.

Grandin, N., Reed, S.I., and Charbonneau, M. (1997). Stn1, a new *Saccharomyces cerevisiae* protein, is implicated in telomere size regulation in association with Cdc13. Genes Dev. **11:** 512–527.

Griffith, J.D., Comeau, L., Rosenfield, S., Stansel, R.M., Bianchi, A., Moss, H., and de Lange, T. (1999). Mammalian telomeres end in a large duplex loop. Cell **97:** 503–514.

Grossi, S., Puglisi, A., Dmitriev, P.V., Lopes, M., and Shore, D. (2004). Pol12, the B subunit of DNA polymerase alpha, functions in both telomere capping and length regulation. Genes Dev. **18:** 992–1006.

Haley, D.A., Horwitz, J., and Stewart, P.L. (1998). The small heat-shock protein, alphaB-crystallin, has a variable quaternary structure. J. Mol. Biol. **277:** 27–35.

Hashimura, Y., and Ueguchi, C. (2011). The Arabidopsis MERISTEM DISORGANIZATION 1 gene is required for the maintenance of stem cells through the reduction of DNA damage. Plant J. **68:** 657–669.

Haslbeck, M., Franzmann, T., Weinfurtner, D., and Buchner, J. (2005). Some like it hot: the structure and function of small heat-shock proteins. Nat. Struct. Mol. Biol. **12:** 842–846.

Heacock, M., Spangler, E., Riha, K., Puizina, J., and Shippen, D.E. (2004). Molecular analysis of telomere fusions in Arabidopsis: multiple pathways for chromosome end-joining. EMBO J. **23:** 2304–2313.

Hendrick, J.P., and Hartl, F.U. (1993). Molecular chaperone functions of heat-shock proteins. Annu. Rev. Biochem. **62:** 349–384.

Holstein, E.M., Clark, K.R., and Lydall, D. (2014). Interplay between nonsense-mediated mRNA decay and DNA damage response pathways reveals that Stn1 and Ten1 are the key CST telomere-cap components. Cell Reports **7:** 1259–1269.

Huang, C., Dai, X., and Chai, W. (2012). Human Stn1 protects telomere integrity by promoting efficient lagging-strand synthesis at telomeres and mediating C-strand fill-in. Cell Res. **22:** 1681–1695.

Jang, H.H., et al. (2004). Two enzymes in one; two yeast peroxiredoxins display oxidative stress-dependent switching from a peroxidase to a molecular chaperone function. Cell **117:** 625–635.

Jun, H.I., Liu, J., Jeong, H., Kim, J.K., and Qiao, F. (2013). Tpz1 controls a telomerase-nonextendible telomeric state and coordinates switching to an extendible state via Ccq1. Genes Dev. **27:** 1917–1931.

Kasbek, C., Wang, F., and Price, C.M. (2013). Human TEN1 maintains telomere integrity and functions in genome-wide replication restart. J. Biol. Chem. **288:** 30139–30150.

Kilian, J., Whitehead, D., Horak, J., Wanke, D., Weinl, S., Batistic, O., D'Angelo, C., Bornberg-Bauer, E., Kudla, J., and Harter, K. (2007). The AtGenExpress global stress expression data set: protocols, evaluation and model data analysis of UV-B light, drought and cold stress responses. Plant J. **50:** 347–363.

Kovalchuk, I., Kovalchuk, O., Kalck, V., Boyko, V., Filkowski, J., Heinlein, M., and Hohn, B. (2003). Pathogen-induced systemic plant signal triggers DNA rearrangements. Nature **423:** 760–762.

Lebel, E.G., Masson, J., Bogucki, A., and Paszkowski, J. (1993). Stress-induced intrachromosomal recombination in plant somatic cells. Proc. Natl. Acad. Sci. USA **90:** 422–426.

Lee, J.R., et al. (2006). Cloning of two splice variants of the rice PTS1 receptor, OsPex5pL and OsPex5pS, and their functional characterization using pex5-deficient yeast and Arabidopsis. Plant J. **47:** 457–466.

Lee, J.R., et al. (2009). Heat-shock dependent oligomeric status alters the function of a plant-specific thioredoxin-like protein, AtTDX. Proc. Natl. Acad. Sci. USA **106:** 5978–5983.

Leehy, K.A., Lee, J.R., Song, X., Renfrew, K.B., and Shippen, D.E. (2013). MERISTEM DISORGANIZATION1 encodes TEN1, an essential telomere protein that modulates telomerase processivity in Arabidopsis. Plant Cell **25:** 1343–1354.

Li, S., Makovets, S., Matsuguchi, T., Blethrow, J.D., Shokat, K.M., and Blackburn, E.H. (2009). Cdk1-dependent phosphorylation of Cdc13 coordinates telomere elongation during cell-cycle progression. Cell **136:** 50–61.

Liu, C.C., Gopalakrishnan, V., Poon, L.F., Yan, T., and Li, S. (2014). Cdk1 regulates the temporal recruitment of telomerase and Cdc13-Stn1-Ten1 complex for telomere replication. Mol. Cell. Biol. **34:** 57–70.

Loayza, D., and De Lange, T. (2003). POT1 as a terminal transducer of TRF1 telomere length control. Nature **423:** 1013–1018.

Lue, N.F., Chan, J., Wright, W.E., and Hurwitz, J. (2014). The CDC13-STN1-TEN1 complex stimulates Pol α activity by promoting RNA priming and primase-to-polymerase switch. Nat. Commun. **5:** 5762.

Lue, N.F., Zhou, R., Chico, L., Mao, N., Steinberg-Neifach, O., and Ha, T. (2013). The telomere capping complex CST has an unusual stoichiometry, makes multipartite interaction with G-Tails, and unfolds higher-order G-tail structures. PLoS Genet. **9:** e1003145.

Lustig, A.J. (2003). Clues to catastrophic telomere loss in mammals from yeast telomere rapid deletion. Nat. Rev. Genet. **4:** 916–923.

Marcand, S., Gilson, E., and Shore, D. (1997). A protein-counting mechanism for telomere length regulation in yeast. Science **275:** 986–990.

McGuffin, L.J., Bryson, K., and Jones, D.T. (2000). The PSIPRED protein structure prediction server. Bioinformatics **16:** 404–405.

Miller, A.S., Balakrishnan, L., Buncher, N.A., Opresko, P.L., and Bambara, R.A. (2012). Telomere proteins POT1, TRF1 and TRF2 augment long-patch base excision repair in vitro. Cell Cycle **11:** 998–1007.

Mitton-Fry, R.M., Anderson, E.M., Theobald, D.L., Glustrom, L.W., and Wuttke, D.S. (2004). Structural basis for telomeric single-stranded DNA recognition by yeast Cdc13. J. Mol. Biol. **338:** 241–255.

Miyagawa, K., et al. (2014). SUMOylation regulates telomere length by targeting the shelterin subunit Tpz1(Tpp1) to modulate shelterin-Stn1 interaction in fission yeast. Proc. Natl. Acad. Sci. USA **111:** 5950–5955.

Miyake, Y., Nakamura, M., Nabetani, A., Shimamura, S., Tamura, M., Yonehara, S., Saito, M., and Ishikawa, F. (2009). RPA-like mammalian Ctc1-Stn1-Ten1 complex binds to single-stranded DNA and protects telomeres independently of the Pot1 pathway. Mol. Cell **36:** 193–206.

Molinier, J., Ries, G., Zipfel, C., and Hohn, B. (2006). Transgeneration memory of stress in plants. Nature **442:** 1046–1049.

Nelson, A.D., and Shippen, D.E. (2012). Surprises from the chromosome front: lessons from Arabidopsis on telomeres and telomerase. Cold Spring Harb. Symp. Quant. Biol. **77:** 7–15.

Nugent, C.I., Hughes, T.R., Lue, N.F., and Lundblad, V. (1996). Cdc13p: a single-strand telomeric DNA-binding protein with a dual role in yeast telomere maintenance. Science **274:** 249–252.

Parikh, D., Fouquerel, E., Murphy, C.T., Wang, H., and Opresko, P.L. (2015). Telomeres are partly shielded from ultraviolet-induced damage and proficient for nucleotide excision repair of photoproducts. Nat. Commun. **6:** 8214.

Peschek, J., Braun, N., Franzmann, T.M., Georgalis, Y., Haslbeck, M., Weinkauf, S., and Buchner, J. (2009). The eye lens chaperone alpha-crystallin forms defined globular assemblies. Proc. Natl. Acad. Sci. USA **106:** 13272–13277.

Peschek, J., Braun, N., Rohrberg, J., Back, K.C., Kriehuber, T., Kastenmüller, A., Weinkauf, S., and Buchner, J. (2013). Regulated structural transitions unleash the chaperone activity of αB-crystallin. Proc. Natl. Acad. Sci. USA **110:** E3780–E3789.

Petreaca, R.C., Chiu, H.C., Eckelhoefer, H.A., Chuang, C., Xu, L., and Nugent, C.I. (2006). Chromosome end protection plasticity revealed by Stn1p and Ten1p bypass of Cdc13p. Nat. Cell Biol. **8:** 748–755.

Prilusky, J., Felder, C.E., Zeev-Ben-Mordehai, T., Rydberg, E.H., Man, O., Beckmann, J.S., Silman, I., and Sussman, J.L. (2005). FoldIndex: a simple tool to predict whether a given protein sequence is intrinsically unfolded. Bioinformatics **21:** 3435–3438.

Qi, H., and Zakian, V.A. (2000). The Saccharomyces telomere-binding protein Cdc13p interacts with both the catalytic subunit of DNA polymerase alpha and the telomerase-associated est1 protein. Genes Dev. **14:** 1777–1788.

Rahavi, M.R., Migicovsky, Z., Titov, V., and Kovalchuk, I. (2011). Transgenerational adaptation to heavy metal salts in Arabidopsis. Front. Plant Sci. **2:** 91.

Raman, B., and Rao, C.M. (1997). Chaperone-like activity and temperature-induced structural changes of alpha-crystallin. J. Biol. Chem. **272:** 23559–23564.

Renfrew, K.B., Song, X., Lee, J.R., Arora, A., and Shippen, D.E. (2014). POT1a and components of CST engage telomerase and regulate its activity in Arabidopsis. PLoS Genet. **10:** e1004738.

Riha, K., McKnight, T.D., Griffing, L.R., and Shippen, D.E. (2001). Living with genome instability: plant responses to telomere dysfunction. Science **291:** 1797–1800.

Saleh, A., Alvarez-Venegas, R., and Avramova, Z. (2008). An efficient chromatin immunoprecipitation (ChIP) protocol for studying histone modifications in Arabidopsis plants. Nat. Protoc. **3:** 1018–1025.

Smogorzewska, A., van Steensel, B., Bianchi, A., Oelmann, S., Schaefer, M.R., Schnapp, G., and de Lange, T. (2000). Control of human telomere length by TRF1 and TRF2. Mol. Cell. Biol. **20:** 1659–1668.

Song, X., Leehy, K., Warrington, R.T., Lamb, J.C., Surovtseva, Y.V., and Shippen, D.E. (2008). STN1 protects chromosome ends in *Arabidopsis thaliana.* Proc. Natl. Acad. Sci. USA **105:** 19815–19820.

Sun, J., Yu, E.Y., Yang, Y., Confer, L.A., Sun, S.H., Wan, K., Lue, N.F., and Lei, M. (2009). Stn1-Ten1 is an Rpa2-Rpa3-like complex at telomeres. Genes Dev. **23:** 2900–2914.

Sun, Y., and MacRae, T.H. (2005). Characterization of novel sequence motifs within N- and C-terminal extensions of p26, a small heat shock protein from *Artemia franciscana.* FEBS J. **272:** 5230–5243.

Surovtseva, Y.V., Churikov, D., Boltz, K.A., Song, X., Lamb, J.C., Warrington, R., Leehy, K., Heacock, M., Price, C.M., and Shippen, D.E. (2009). Conserved telomere maintenance component 1 interacts with STN1 and maintains chromosome ends in higher eukaryotes. Mol. Cell **36:** 207–218.

Surovtseva, Y.V., Shakirov, E.V., Vespa, L., Osbun, N., Song, X., and Shippen, D.E. (2007). Arabidopsis POT1 associates with the telomerase RNP and is required for telomere maintenance. EMBO J. **26:** 3653–3661.

Swamy-Mruthinti, S., Srinivas, V., Hansen, J.E., and Rao, ChM. (2013). Thermal stress induced aggregation of aquaporin 0 (AQP0) and protection by α-crystallin via its chaperone function. PLoS One **8:** e80404.

Tang, G., Peng, L., Baldwin, P.R., Mann, D.S., Jiang, W., Rees, I., and Ludtke, S.J. (2007). EMAN2: an extensible image processing suite for electron microscopy. J. Struct. Biol. **157:** 38–46.

Teixeira, M.T., Arneric, M., Sperisen, P., and Lingner, J. (2004). Telomere length homeostasis is achieved via a switch between telomerase- extendible and -nonextendible states. Cell **117:** 323–335.

Tompa, P., and Csermely, P. (2004). The role of structural disorder in the function of RNA and protein chaperones. FASEB J. **18:** 1169–1175.

Wang, F., Stewart, J.A., Kasbek, C., Zhao, Y., Wright, W.E., and Price, C.M. (2012). Human CST has independent functions during telomere duplex replication and C-strand fill-in. Cell Reports **2:** 1096–1103.

Wang, R.C., Smogorzewska, A., and de Lange, T. (2004). Homologous recombination generates T-loop-sized deletions at human telomeres. Cell **119:** 355–368.

Xu, L., Petreaca, R.C., Gasparyan, H.J., Vu, S., and Nugent, C.I. (2009). TEN1 is essential for CDC13-mediated telomere capping. Genetics **183:** 793–810.

Zhang, Y., Chen, L.Y., Han, X., Xie, W., Kim, H., Yang, D., Liu, D., and Songyang, Z. (2013). Phosphorylation of TPP1 regulates cell cycle-dependent telomerase recruitment. Proc. Natl. Acad. Sci. USA **110:** 5457–5462.